Simultaneous WiFi Ranging Compensation and Localization for Indoor NLoS Environments

Meng Sun, Yunjia Wang, Lu Huang, Shenglei Xu, Hongji Cao,
Wout Joseph and David Plets

***Abstract*— Smartphone-based WiFi ranging using fine time measurement (FTM) is severely impacted by Non-line-of-sight (NLoS) environments, which causes significant positioning errors. To address this problem, we propose a novel WiFi FTM positioning (WFP) approach based on the geomagnetism and enhanced genetic algorithm (EGA), which can simultaneously execute WiFi localization and ranging compensation. Based on the distribution of the ranging error in NLoS environments, a semiparametric error model-based ranging compensation method is proposed. To construct the EGA searching model, geomagnetism-based positioning is adopted and fed to the EGA together with the measured WiFi ranging data and the ranging compensation method. During online localization, the EGA model dynamically compensates for the erroneous ranging data until it finds the optimal position. Experimental results show that the ranging and localization accuracy of this EGA-based WFP are 1.33 m and 1.64 m, being an improvement of 30.7% and 56.5% compared to the uncompensated ranging data and the trilateration algorithm using the weighted least square (WLS) method, respectively.**

***Index Terms*— Indoor localization, WiFi FTM, ranging compensation, geomagnetism, NLoS, enhanced genetic algorithm.**

I. Introduction

WIFI FTM-based localization has attracted extensive attention. In Line-of-sight (LoS) environments, smartphone-based WiFi FTM ranging can achieve meter-level accuracy [1]. However, more complex indoor environments lead to serious ranging errors. To improve precision, different methods have been developed, such as using NLoS/LoS identification [2], designing an optimization strategy [3], and integrating map information [4], WiFi received signal strength (RSS) [5], or pedestrian dead reckoning (PDR) with WFP [6], [7]. The NLoS/LoS detection in [2] is to clarify the characteristics of the measured WiFi data in LoS/NLoS conditions and then eliminate the NLoS data to realize accuracy improvement. Algorithm optimization comprises strategies (e.g. the temporal-spatial constraint strategy [3]) to limit the influence of ranging errors on the localization results. The sensor fusion method integrates PDR and WFP based on the extended Kalman filter [6], or unscented Kalman filter [7]. The poor performance of WFP is improved with the fusion of PDR, but the WiFi ranging problem itself is not well addressed.

High-accuracy WiFi ranging is the basis of the high-accuracy WFP, making the construction of an efficient WiFi ranging model very essential. In [7], a ranging compensation model considering the clock deviation, NLoS, and multipath factors is proposed. In [6] and [8], the relationship between the ranging error and distance is considered as parametric and fitted by using the least square (LS) and nonlinear least square (NLS). But these parametric models do not work well in NLoS conditions. In [5], the RSS-based range and the FTM-based range are integrated based on the Kalman filter. The reported ranging accuracy is meter-level in an open outdoor area. In [9], the "FUSIC" method is proposed to extend the accuracy of WiFi ranging in LoS conditions to NLoS settings by using the channel state information, which is not readily available on smartphones. An efficient smartphone-based WiFi ranging model for localization in NLoS environments is still lacking.

To address the poor performance of WiFi ranging and positioning, we study the characteristics of the ranging errors and construct a semiparametric error model-based ranging compensation method. Based on this, we use an EGA to search for the optimal position and ranging errors compensation terms. For the EGA implementation, we take the geomagnetism-based positioning (GP) to generate the initial population of EGA for evolution, given the good performance of GP in NLoS environments [10]. Our contributions are as follows:

1) We analyze the characteristics of WiFi ranging errors in NLoS environments and build a semiparametric ranging error model, which describes the ranging error distribution and improves the ranging accuracy.
2) We propose a novel geomagnetism/EGA-based WFP approach that can simultaneously search for the optimal WiFi position and compensate for the ranging data.
3) We conduct extensive experiments to evaluate the proposed methods and confirm that this EGA-based WFP improves the accuracy of ranging and localization.

II. Algorithm Architecture

Fig. 1 shows the flow graph of the geomagnetism/ EGA-based WFP approach. Offline, based on the measured WiFi FTM data, a semiparametric ranging error model and a WiFi ranging model are built. Online, the WLS method is used to estimate a coarse-grained WiFi position, which reduces the searching space of GP. The GP using an enhanced mind evolutionary algorithm (EMEA) is adopted for magnetic position estimation. A set of grid points around this magnetic

This work was supported by the National Key Research and Development Program of China under Grant 2016YFB0502102, in part by the China Scholarship Council under Grant CSC 202006420023. The associate editor coordinating the review of this letter and approving it for publication was S. Bartoletti.

(Corresponding author: Yunjia Wang.)

Meng Sun, Yunjia Wang, Shenglei Xu, and Hongji Cao are with the Key Laboratory of Land Environment and Disaster Monitoring, MNR, School of Environment and Spatial Informatics, China University of Mining and Technology, Xuzhou 221116, China (e-mail: msun@cumt.edu.cn; wyjc411@163.com; cumtxsl@cumt.edu.cn; hjcao@cumt.edu.cn).

Lu Huang is with the State Key Laboratory of Satellite Navigation System and Equipment Technology, Shijiazhuang 050081, China (e-mail: hlcetc54@163.com).

Wout Joseph and David Plets are with the WAVES Group, Department of Information Technology, Ghent University—imec, 9052 Ghent, Belgium (e-mail: wout.joseph@ugent.be; david.plets@ugent.be).

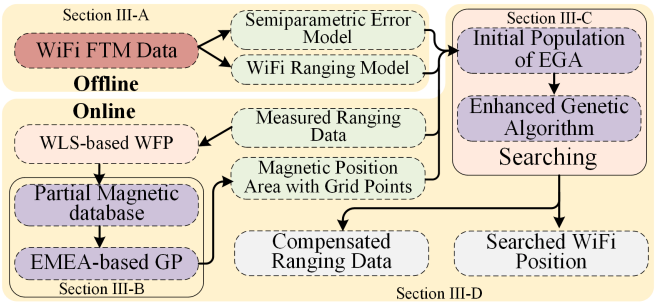

Fig. 1. Flow graph of the proposed method.

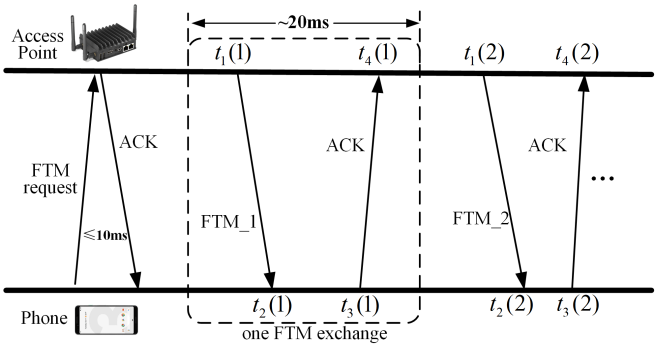

Fig. 2. WiFi FTM producer.

position is selected, and then provided for the population initialization of EGA. Finally, the ranging error model, WiFi ranging model, measured ranging data, and the grid point set are fed to the EGA. After that, EGA starts searching until meeting the convergence condition. The compensated ranging data and the searched optimal position are obtained as the final results.

III. Methods

A. WiFi FTM Localization and Ranging Error Model

1) WiFi FTM Ranging and Localization: As Fig. 2 shows, the initial FTM response is completed via the access point (AP) responds to the FTM request by sending an acknowledge (ACK) message to the phone. After this, the FTM and ACK exchanging starts. The time-of-departure (ToD) $t_1(1)$ and the time-of-arrival (ToA) $t_2(1)$ of the FTM package are recorded by the AP and phone. And then, the TOD $t_3(1)$ and TOA $t_4(1)$ of the ACK package are captured by phone and AP, respectively. If n successful exchanges are completed, the theoretical WiFi ranging model is defined as follows:

$$d = \frac{C}{2n}\sum_{k=1}^{n}([t_4(k) - t_1(k)] - [t_3(k) - t_2(k)]) \tag{1}$$

where d is the theoretical distance, C is the light speed.

If there are n APs and $n \geq 3$, the phone's 2D position can be estimated using the WLS method as follows:

$$\boldsymbol{X} = (\boldsymbol{A}^T\boldsymbol{P}\boldsymbol{A})^{-1}\boldsymbol{A}^T\boldsymbol{P}\boldsymbol{L} \tag{2}$$

where $\boldsymbol{X}$ represents the estimated 2D position, $\boldsymbol{P}$ is the weight matrix and relates to the measured distances, $\boldsymbol{A}$ and $\boldsymbol{L}$ are defined using the coordinates of APs and the measured distances, respectively. The detailed calculation methods of $\boldsymbol{A}$, $\boldsymbol{P}$ and $\boldsymbol{L}$ can be found in [6].

2) Ranging and Error Model: Hardware, NLoS, multipath and clock deviation factors lead to errors in WiFi ranging [7].

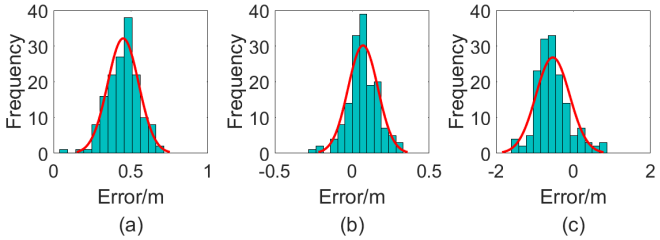

Fig. 3. Distributions of e at different ground-truth distances in NLoS environments. (a) 3.6 m, (b) 6 m, (c) 10 m.

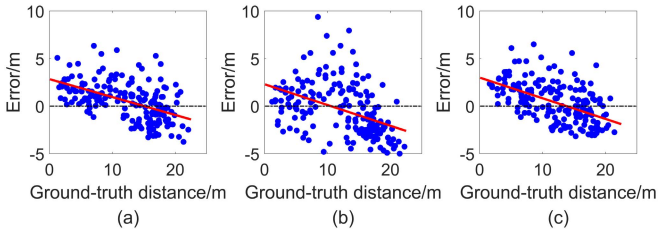

Fig. 4. Distributions of e of different APs at different ground-truth distances in NLoS environments. (a) No.1 AP, (b) No.2 AP, (c) No.3 AP.

Considering these factors, a real-time WiFi ranging compensation model is defined as:

$$\hat{d} = d + d_h + d_c + d_{nlos} + d_m + \epsilon \tag{3}$$

where $\hat{d}$ and d are the measured and theoretical distances, respectively; ϵ is a random error, d_h is the initial deviation error caused by the hardware and can be calibrated using the difference between the ground-truth distance (e.g. 1 m) and the measured distance; d_c, d_{nlos} and d_m are the errors caused by random clock deviation, NLoS, and multipath factors, respectively. These three errors and ϵ reflected in the measured data can be considered as a sum error e, (3) is written as:

$$\hat{d} = d + d_h + e \tag{4}$$

The problem is to find the characteristics of the sum error e. To make analyses, we measured WiFi ranging data at different ground-truth points in an NLoS environment (defined in *Section* IV.A), where the WiFi ranging is always affected by concrete and glass walls. The ranging errors distributions are shown in Fig. 3 and Fig. 4. which reveal that ranging errors conform to the Gaussian distribution (might be positive or negative) at a given distance, and have a descending trend as the distance increases. Moreover, Fig. 4 shows that the red trendlines are similar and independent of different APs.

We summarize the characteristic of e as having a linear relationship with the distance between the AP and phone, and also having a nonlinear random term (Gaussian distribution). This characteristic can be described using the semi-parametric model [11]. If there are n APs, the model is defined as:

$$\boldsymbol{E}_{n\times 1} = \boldsymbol{B}_{n\times 2}\boldsymbol{x}_{2\times 1} + \boldsymbol{S}_{n\times 1} + \Delta \tag{5}$$

where $\boldsymbol{E}$ is the matrix of measured errors for the n APs, $\boldsymbol{E} = [e_1, e_2, \ldots, e_n]^{\mathrm{T}}$, $\boldsymbol{B}$ is the non-singular matrix, which consists of the measured distances for all APs; $\boldsymbol{x}$ is the parameter matrix; $\boldsymbol{B}\boldsymbol{x}$ describes the linear relationship (trendlines in Fig. 4); $\boldsymbol{S}$ represents the nonlinear random character (Gaussian distribution), $\boldsymbol{S} = [s_1, s_2, \ldots, s_n]^{\mathrm{T}}$, Δ is the measurement noise, respectively. The error equation of (5) is defined as:

$$\boldsymbol{V}_{n\times 1} = \boldsymbol{B}_{n\times 2}\hat{\boldsymbol{x}}_{2\times 1} + \boldsymbol{S}_{n\times 1} - \boldsymbol{E}_{n\times 1} \tag{6}$$

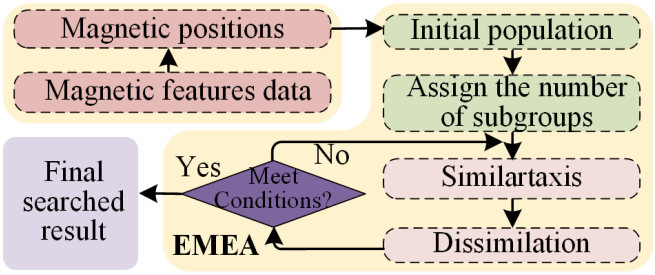

Fig. 5. Flowchart of the EMEA-based GP.

where $\boldsymbol{V}$ is the difference of $(\boldsymbol{B}\hat{\boldsymbol{x}} + \boldsymbol{S})$ and $\boldsymbol{E}$, $\hat{\boldsymbol{x}}$ is the matrix that contains the optimal linear parameters, which are the results of the mathematical operation of $\boldsymbol{B}$, $\boldsymbol{S}$, and $\boldsymbol{E}$, making $\boldsymbol{V}$ obtain the minimal value. The number of the uncertain parameters in (5) is $(n+2)$, while there are only n measurements. Based on the penalized least squares estimation [12], to estimate the optimal parameters, (7) should be met:

$$min(\boldsymbol{V}^{\mathrm{T}}\boldsymbol{P}\boldsymbol{V} + \alpha \boldsymbol{S}^{\mathrm{T}}\boldsymbol{R}\boldsymbol{S}) \tag{7}$$

where $\boldsymbol{P}$ and $\boldsymbol{R}$ are the positive-definite matrices, α is the scale factor, respectively. To obtain the minimal value of (7), we can construct a Lagrange function as follows:

$$\Psi = \boldsymbol{V}^{\mathrm{T}}\boldsymbol{P}\boldsymbol{V} + \alpha \boldsymbol{S}^{\mathrm{T}}\boldsymbol{R}\boldsymbol{S} - 2\boldsymbol{K}^{\mathrm{T}}(\boldsymbol{B}\hat{\boldsymbol{x}} + \boldsymbol{S} - \boldsymbol{E} - \boldsymbol{V}) \tag{8}$$

then making $\frac{\partial \Psi}{\partial \boldsymbol{V}}$, $\frac{\partial \Psi}{\partial \boldsymbol{S}}$, $\frac{\partial \Psi}{\partial \hat{\boldsymbol{x}}}$ equal to 0, we obtain:

$$\boldsymbol{K} = \boldsymbol{P}\boldsymbol{V} \tag{9}$$

$$\boldsymbol{K} = -\alpha \boldsymbol{R}\boldsymbol{S} \tag{10}$$

$$\boldsymbol{B}^{\mathrm{T}}\boldsymbol{K} = 0 \tag{11}$$

combining (6), (9), and (11), we get:

$$\boldsymbol{B}^{\mathrm{T}}\boldsymbol{P}\boldsymbol{B}\hat{\boldsymbol{x}} + \boldsymbol{B}^{\mathrm{T}}\boldsymbol{P}\boldsymbol{S} - \boldsymbol{B}^{\mathrm{T}}\boldsymbol{P}\boldsymbol{E} = 0 \tag{12}$$

making $\boldsymbol{B}^{\mathrm{T}}\boldsymbol{P}\boldsymbol{B} = \boldsymbol{N}$, $\hat{\boldsymbol{x}}$ is calculated as follows:

$$\hat{\boldsymbol{x}} = \boldsymbol{N}^{-}1\boldsymbol{B}^{\mathrm{T}}\boldsymbol{P}\boldsymbol{E} - \boldsymbol{N}^{-}1\boldsymbol{B}^{\mathrm{T}}\boldsymbol{P}\boldsymbol{S} \tag{13}$$

combining (6), (9), (10), and (12), $\boldsymbol{S}$ is calculated as:

$$\boldsymbol{S} = (\boldsymbol{P} + \alpha\boldsymbol{R} - \boldsymbol{P}\boldsymbol{B}\boldsymbol{N}^{-}1\boldsymbol{B}^{\mathrm{T}}\boldsymbol{P})(\boldsymbol{P} - \boldsymbol{P}\boldsymbol{B}\boldsymbol{N}^{-}1\boldsymbol{B}^{\mathrm{T}}\boldsymbol{P})\boldsymbol{E} \tag{14}$$

For online usage, the initial ranging error terms are first estimated based on the linear relationship. Then, the optimal $\hat{\boldsymbol{x}}$ and $\boldsymbol{S}$ are calculated by using (13) and (14), respectively. The final ranging error terms are obtained based on (5).

B. Geomagnetism-Based Positioning Using EMEA

It has been proved that the EMEA-based GP performs well in NLoS environments [10]. In this letter, we adopted this EMEA-based GP to initialize the population of EGA. Before executing GP, a division of the positioning area is first made. As Fig.5 shows, based on the high sampling rate of the magnetometer (e.g. 50 Hz), many temporary magnetic positions are obtained and used for the EMEA's evolution process, which adopts the similartaxis and dissimilation operators to find the optimal true magnetic position. Then, an area with a radius of 5 m around this position is selected and the grid points within this area constitute the initial population for EGA searching.

C. Enhanced Genetic Algorithm

1) Selection Strategy: After the population initialization, every individual is assigned a fitness value and a special chromosome (will be defined in *Section* III.D). EGA selects the best individuals based on their fitness. The larger the fitness value of an individual, the higher the probability of being selected, which is defined as follows:

$$p_i = \frac{f(x_i)}{\sum_{j=1}^{N} f(x_j)} \qquad j = 1, 2, \ldots, N \tag{15}$$

where p_i is the probability of being selected, N is the number of individuals, $f(x_i)$ is the individual's fitness. The roulette-wheel selection method [13] is used to evaluate whether to execute selection if (16) is met:

$$p_i > s \qquad \forall p_i, s \in [0, 1] \tag{16}$$

where s is a random number. During the execution process, the individual with best fitness is first selected.

2) Adaptive Crossover Strategy: Crossover creates new offspring by exchanging genes from the selected individuals' chromosomes. Before performing crossover, two individuals and the crossover points on the chromosomes are first selected. Then, given a crossover probability p_c and random number r, the genes at the corresponding positions are exchanged if p_c and r satisfy (17):

$$p_c > r \qquad \forall p_c, r \in [0, 1] \tag{17}$$

As the evolution progresses, gene exchanging should be easier within the population because more good individuals are generated. Adaptive crossover strategy can dynamically assign the crossover probability and the definition is as follows:

$$p_c = p_{cmax} - \frac{n \times (p_{cmax} - p_{cmin}) \times \bar{f}_i - m}{m \times \bar{f}_i} \tag{18}$$

where p_{cmax} and p_{cmin} are the maximal and minimal crossover probabilities, which are set as 0.5 and 0.1 in this work, $\bar{f}_i$ is the average fitness value of the $i-th$ generation, m and n are the maximal and current iteration numbers of the evolution, respectively.

3) Adaptive Mutation Strategy: For the mutation execution, the locations of mutation on the chromosomes are first randomly selected. After that, with a mutation probability p_m and a random number t, the genes at the corresponding positions are mutated if p_m and t satisfy (19):

$$p_m > t \qquad \forall p_m, t \in [0, 1] \tag{19}$$

Mutation might generate good or bad genes, but bad genes affect the evolution process, which means that mutation with a constant probability slows down the convergence speed of EGA. Therefore, an adaptive mutation strategy is adopted to dynamically set the mutation probability during the evolution process, and the definition is as follows:

$$p_m = p_{mi} - \frac{n \times (p_{mi} - p_{mmin}) \times \bar{f}_i - m}{m \times \bar{f}_i} \tag{20}$$

where p_{mi} and p_{mmin} are the initial and minimal mutation probabilities, which are set as 0.4 and 0.1, $\bar{f}_i$ is the average fitness value of the $i-th$ generation, m and n are maximal and the current iteration numbers of the evolution, respectively.

D. Simultaneous WiFi FTM Localization and Ranging Compensation Based on EGA

To construct the EGA model, the first problem is how to express an individual's chromosome. The grid points in *Section B* and the ranging errors estimated by the error model

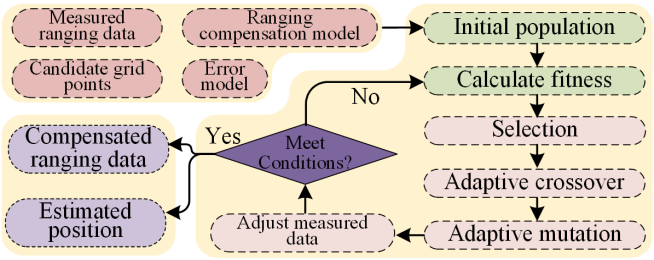

Fig. 6. Flowchart of the EGA-based WFP.

in *Section A* are used to define chromosomes as:

$$chrom = [x_i, y_i, e_1, e_2, \ldots, e_n] \tag{21}$$

where x_i and y_i are coordinate values of the grid points, e_i is the ranging error from the $i-th$ AP, $i = 1, 2, \ldots, n$. After that, the key problem is to find a good fitness function. In theory, if there are no ranging errors, the measured distance (MD) equals the ground-truth plane distance (PD) between the phone and AP. Considering the error compensation terms, this relationship can be expressed as:

$$\zeta_i = \hat{d}_i - d_{hi} - e_i - \sqrt{(x - x_{Ri})^2 + (y - y_{Ri})^2} \approx 0 \tag{22}$$

where ζ_i is the difference of MD and PD, (x, y) and (x_{Ri}, y_{Ri}) are the true coordinates of the phone and $i-th$ AP, respectively. If there are n APs, (22) is expressed as:

$$\begin{bmatrix} \zeta_1 \\ \zeta_2 \\ \cdots \\ \zeta_n \end{bmatrix} = \begin{bmatrix} \hat{d}_1 - d_{h1} - e_1 \\ \hat{d}_2 - d_{h2} - e_2 \\ \cdots \\ \hat{d}_n - d_{hn} - e_n \end{bmatrix} - \begin{bmatrix} \sqrt{(x - x_{R1})^2 + (y - y_{R1})^2} \\ \sqrt{(x - x_{R2})^2 + (y - y_{R2})^2} \\ \cdots \\ \sqrt{(x - x_{Rn})^2 + (y - y_{Rn})^2} \end{bmatrix} \tag{23}$$

The optimal position and error compensation terms make the left term of (23) get the minimal value. This relationship is the fitness function:

$$f = \frac{1}{\sum_{i=1}^{n} |\zeta_i|} \tag{24}$$

Based on (21) and (24), the individuals' fitness is obtained. Then, the measured ranging data, the initialized population, error model and ranging compensation model are fed to EGA, and evolution starts. When EGA finishes one-time searching, the error compensation terms are obtained by decoding the chromosome of the best individual. Then, based on these errors, the measured ranging data is adjusted by using (4). If the number of iterations reaches 50, EGA meets the convergence condition and the best individual of the final iteration is decoded. The WiFi position and compensated ranging data are outputted. The detailed process is shown in Fig. 6.

IV. Experiments

A. Experimental Setup

All the experiments were conducted in the second floor of the state key laboratory of satellite navigation system and equipment technology (Shijiazhuang, China). 8 Compulab WILD APs are installed outside the second floor. The concrete and glass walls block the WiFi signal propagation path and APs cannot be directly observed from the corridors or rooms, making the NLoS condition. Fig. 7(a) shows that 166 reference points (RP) with a separation of 1.2 m are selected and interpolated into 1756 points. The magnetic features are collected at these RPs and linearly interpolated. A Pixel 3 phone (Fig. 7(b)) with developed software that can simultaneously measure the magnetic features and WiFi data with the sampling rates of 50 Hz and 5 Hz, respectively. The testing data are collected three times at 64 testing points. A laptop with 8 GB RAM and a 2.6GHz CPU is used for the data analysis.

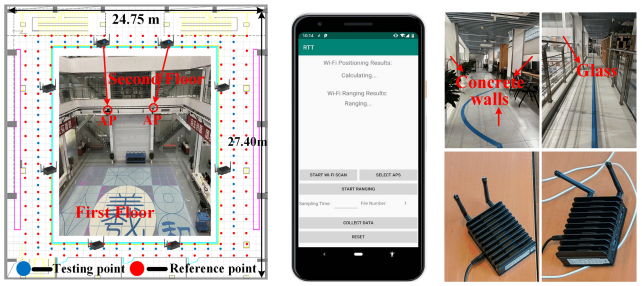

Fig. 7. Experimental setup. (a) Floor plan, (b) Pixel 3 phone, (c) Access points and the real scenarios of the second floor.

TABLE I
Absolute Errors and MET Comparison of Different Models

Algorithm	Max/m	Mean/m	RMSE/m	75%Error/m	MET/ms
Uncompensated	13.23	1.93	2.47	2.67	/
LS	14.33	1.83	2.36	2.72	0.28
NLS	14.19	1.84	2.37	2.69	0.21
RSS-FTM	6.58	1.76	2.19	2.58	0.47
Semi Only	7.56	1.62	2.04	2.32	0.66
Semi with EGA	6.49	1.33	1.72	1.95	284.3

B. WiFi Ranging Compensation Analysis

We denote the proposed ranging method as "Semi with EGA" and compare it to the RSS-FTM fusion [5], LS [6], NLS [8]. The method only using the semiparametric model without EGA is denoted as "Semi Only". All the ranging models are built based on the same ranging errors datasets. They are calculated by using the measured ranging data on 188 modeling points and the ground-truth distances between modeling points and access points.

Tab. I shows the mean absolute ranging error and mean execution time (MET) of different methods. The mean absolute ranging error of the uncompensated data is about 1.93 m, which can be improved by adopting the LS, NLS, and RSS-FTM methods, albeit with an improvement within 0.2 m (10.4%). LS and NLS models obtain very similar results. The mean ranging accuracy of only using the semi-parametric model is 1.62 m, which is further improved to 1.33 m after applying the EGA, with an accuracy improvement percentage (ACP) of about 30.7%. Using the semiparametric model with EGA has the best ACP. The same conclusion can be drawn when comparing the root-mean-square errors (RMSE) of these models. Fig. 8 reveals the cumulative distribution functions of ranging errors and clearly shows that our method has the best performance. For the MET comparison, our method consumes more time to complete ranging compensation. However, it can still deliver results within 0.3 s. This means that our method will allow for real-time processing when deploying on smartphones.

C. WiFi Positioning Methods Comparison

We denote the proposed localization method as "EGA-WFPG", and compare it to the approaches of WLS [6],

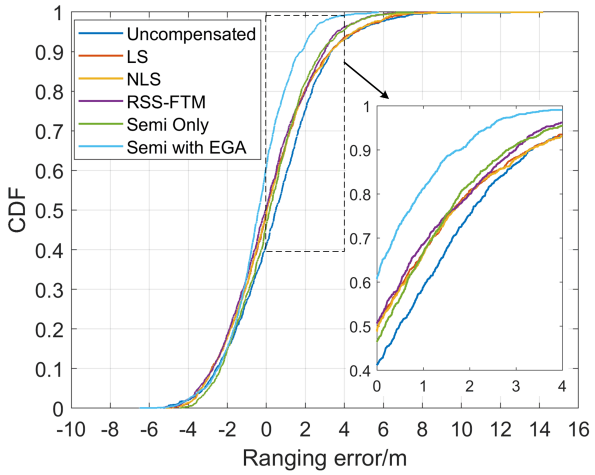

Fig. 8. CDFs comparison of ranging errors of different methods.

TABLE II

ERRORS COMPARISON OF WIFI POSITIONING ALGORITHMS

Algorithm	Min/m	Max/m	Mean/m	RMSE/m	75%Error/m
WLS	0.37	11.20	3.77	4.37	5.09
RSS-FTM	0.32	11.35	3.25	3.74	4.17
EMEA-WLS	0.10	5.43	1.82	2.08	2.51
EGA-WFPW	0.20	12.47	2.21	2.77	2.74
EGA-WFPG	0.08	5.18	1.64	1.89	2.14

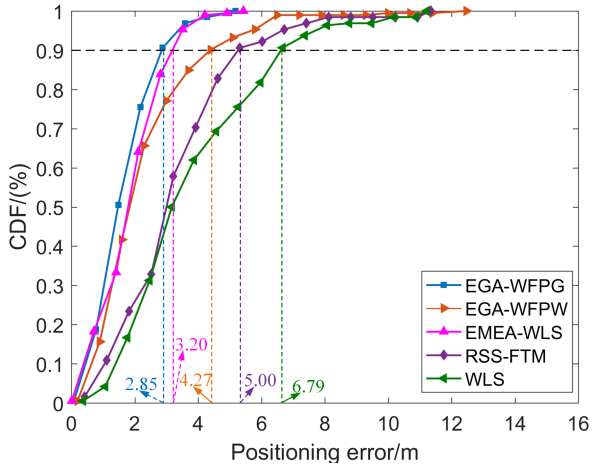

Fig. 9. CDFs comparison of positioning errors of different methods.

RSS-FTM [5], EMEA-WLS [10]. To make a better comparison, we implement the WFP using the WiFi positions for the population generation of the EGA and denote it as "EGA-WFPW". Tab. II shows that the mean accuracy and RMSE of EGA-WFPG are 1.64 m and 1.89 m, which are improved by 56.5% and 56.8 % compared with the WLS, and are better than those of the EMEA-WLS, RSS-FTM, and EGA-WFPW. These results show that the proposed EGA-WFPG has high accuracy and better stability. For a confidence level of 75%, EGA-WFPG obtains the best accuracy of 2.14 m. Based on this experimental analysis, we conclude that this EGA-WFPG method can perform well in NLoS environments.

D. Positioning Methods Discussion

Compared to the state-of-the-art approaches of RSS-FTM [5], WLS [6], and EMEA-WLS [10], the proposed EGA-WFPG obtains the best localization accuracy, RMSE, and ACP. Fig. 9 reveals that the EGA-WFPG obtains a localization accuracy of 2.85 m in 90% of the cases, which is better than that of the other four methods. Fig. 9 also reveals the better performance of EGA-WFPG under different confidence levels compared to others methods. Although using NLoS/LoS identification can also improve accuracy in [2], the reported ACP is only 36.4%, while the ACP of EGA-WFPG is 56.5%. Different from previous works [5], [6], and [8], which only calibrate the ranging data once before executing the localization algorithm, our method can dynamically adjust the measured ranging data using the EGA based on the semiparametric error model and ranging model. The estimated WiFi position and compensated ranging data are simultaneously obtained after EGA searching. All the experimental results demonstrate that the proposed EGA-WFPG method is an efficient approach for limiting the NLOS influence on localization accuracy.

V. CONCLUSION

In this letter, we propose a novel WiFi FTM positioning approach for NLoS scenarios localization based on geomagnetism and EGA. Experiments reveal that the mean ranging compensation and positioning accuracy of the proposed WFP are 1.33 m and 1.64 m, which are improved by about 30.7% and 56.5%, respectively, compared to the classic WLS. In the future, we will study the fusion positioning with the integration of smartphone built-in sensors to improve precision.

REFERENCES

[1] Y. Yu, R. Chen, Z. Liu, G. Guo, F. Ye, and L. Chen, "Wi-Fi fine time measurement: Data analysis and processing for indoor localisation," *J. Navigat.*, vol. 73, no. 5, pp. 1106–1128, Sep. 2020.

[2] M. Si, Y. Wang, S. Xu, M. Sun, and H. Cao, "A Wi-Fi FTM-based indoor positioning method with LOS/NLOS identification," *Appl. Sci.*, vol. 10, no. 3, p. 956, Feb. 2020.

[3] W. Shao, H. Luo, F. Zhao, H. Tian, S. Yan, and A. Crivello, "Accurate indoor positioning using temporal–spatial constraints based on Wi-Fi fine time measurements," *IEEE Internet Things J.*, vol. 7, no. 11, pp. 11006–11019, Nov. 2020.

[4] L. Banin, U. Schatzberg, and Y. Amizur, "WiFi FTM and map information fusion for accurate positioning," in *Proc. IPIN*, 2016, pp. 1–4.

[5] G. Guo, R. Chen, F. Ye, X. Peng, Z. Liu, and Y. Pan, "Indoor smartphone localization: A hybrid WiFi RTT-RSS ranging approach," *IEEE Access*, vol. 7, pp. 176767–176781, 2019.

[6] M. Sun, Y. Wang, S. Xu, H. Qi, and X. Hu, "Indoor positioning tightly coupled Wi-Fi FTM ranging and PDR based on the extended Kalman filter for smartphones," *IEEE Access*, vol. 8, pp. 49671–49684, 2020.

[7] Y. Yu, R. Chen, L. Chen, G. Guo, F. Ye, and Z. Liu, "A robust dead reckoning algorithm based on Wi-Fi FTM and multiple sensors," *Remote Sens.*, vol. 11, no. 5, p. 504, 2019.

[8] H. Cao, Y. Wang, J. Bi, S. Xu, M. Si, and H. Qi, "Indoor positioning method using WiFi RTT based on LOS identification and range calibration," *ISPRS Int. J. Geo-Inf.*, vol. 9, no. 11, p. 627, Oct. 2020.

[9] K. Jiokeng, G. Jakllari, A. Tchana, and A.-L. Beylot, "When FTM discovered MUSIC: Accurate WiFi-based ranging in the presence of multipath," in *Proc. IEEE INFOCOM - IEEE Conf. Comput. Commun.*, Jul. 2020, pp. 1857–1866.

[10] M. Sun *et al.*, "Geomagnetic positioning-aided Wi-Fi FTM localization algorithm for NLOS environments," *IEEE Commun. Lett.*, vol. 26, no. 5, pp. 1022–1026, May 2022, doi: 10.1109/LCOMM.2022.3155929.

[11] J. L. Powell, "Estimation of semiparametric models," in *Handbook Econometrics*, vol. 4. Amsterdam, The Netherlands: Elsevier, 1994, pp. 2443–2521.

[12] P. J. Green and B. W. Silverman, *Nonparametric Regression Generalized Linear Models: A Roughness Penalty Approach*. Boca Raton, FL, USA: CRC Press, 2019.

[13] K. Jebari and M. Madiafi, "Selection methods for genetic algorithms," *Int. J. Emerg. Sci.*, vol. 3, no. 4, pp. 333–344, Dec. 2013.